Proceeding of the 15th International Forum of Automotive Traffic Safety, 2018, pp 287-294
No.ATS.2018.414

Research on the Injury Risk of 6YO Child Occupant in Small Overlap Frontal Impact

Bin TANG [1, 2], Yong HAN [1, 2, 3], Yu WANG [1], Hongwu Huang [1, 2], Yi YU [1]

1. Xiamen University of Technology, Xiamen, China, 361024, E-mail:yonghan@xmut.edu.cn

2. Fujian Collaborative innovation center for R&D of coach and special vehicle, Xiamen 361024, China

3. State Key Laboratory of Vehicle NVH and Safety Technology, Chongqing;

Abstract: The small overlap frontal impact is a very common type of traffic accidents and causes heavy injury especially for child occupant. The injury risk of 6YO child occupant in small overlap frontal impact was investigated by using finite element (FE) simulation, based on the IIHS Small Overlap Frontal Crashworthiness Evaluation Crash Protocol (Version VI). In which, Taurus FE model, a booster FE model and THUMS 6YO were used. The result shows that occupant's feet contacted the back of the frontal seat and the door interior and left hand also contacted the door interior in high-backed and backless situations. However, submarining appeared in backless situation. The injury risk of head was low and the risk of rib fracture, heart contusion and lung contusion was high in both situations. Moreover, the injury risk of the head and chest in backless situation was higher than high-backed situation.

Keywords: small overlap frontal impact, THUMS 6YO, booster seat

1 Introduction

Among many types of traffic accidents, frontal impact is the most probable one. And small overlap frontal impact accounts for a high proportion in frontal impact accidents, about 48% [1]. At the same time, occupant injuries or deaths caused by small overlap frontal impact are more serious than other types of traffic accidents [2]. That the lateral acceleration produced by offset impact will cause the diver-side occupant to hit the door interior may result in a heavy injury [3]. For child occupants, they will afford high injury risk in small overlap frontal impact even though CRS is used. A survey shows that the proportions of head injury and chest injury are 46% and 53% in all parts of body in frontal impacts [4]. In small overlap frontal impact, the head may contact the door interior because of lateral acceleration and the chest will be pressed heavily by seatbelt if child occupant would be restrained by seatbelt.

2 Finite Element Model

In this paper, the vehicle FE model Taurus (Figure 1) which was developed by The National Crash Analysis Center in 2012 is used. The Taurus FE model is 1740Kg and has 921793 nodes, 973329 elements. THUMS 6YO (THUMS 6YO Occupant Model Academic Version 4) (Figure 2) was developed by TOYOTA Central R&D, Inc. CRS FE model (Figure 3) was established based on the booster seat Kidfix XP geometric model provided from Britax Company. The Kidfix XP FE model has 152958 nodes and 286117 elements.

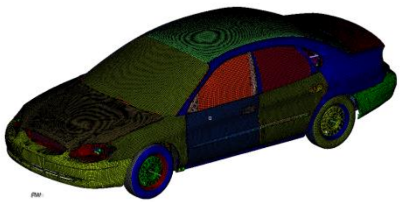

Figure 1 Taurus FE

Figure 2 THUMS 6YO

Figure 3 Kidfix XP FE

25% overlap frontal impact FE model (Figure 4) was built according to IIHS Small Overlap Frontal Crashworthiness Evaluation Crash Protocol (Version VI). The vehicle initial velocity is 64.4 Km/h. THUMS 6YO and Kidfix XP were placed on the driver-side rear seat. The Kidfix XP and the Taurus were connected by ISOFIX, THUMS 6YO was restrained by 3 points belt. The lap belt went through the belt guide hook on the cushion and the shoulder belt went through the belt guide hook on the headrest.

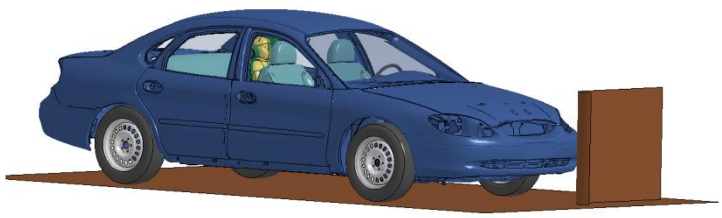

Figure 4 Small Overlap Frontal Impact FE Model

3 Matrix

The table 1 shows the simulation matrix in this paper.

Table 1

NO.	CRS	Fixed Mode
1	High-backed	ISOFIX+3 points belt
2	Backless	ISOFIX+3 points belt

4 Results

4.1 Vehicle Acceleration

What the Figure 5 shows is the time history curves of the vehicle B pillar longitudinal acceleration in high-backed and backless situations. It is obvious that two acceleration curves are similar. Since the vehicle acceleration in each simulation is similar, the loads applied to the occupants are likely to be similar in the two simulations.

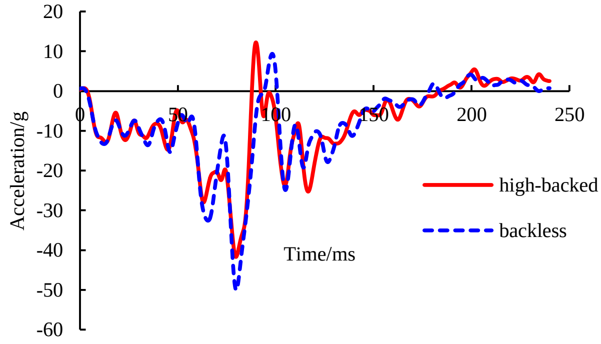

Figure 5 Vehicle Longitudinal Acceleration

4.2 Occupant Kinematic Response

Figure 6 shows that the occupant different postures at the same time intervals in high-backed situation when the small overlap frontal impact was conducting. The obvious rotation could be seen from the vehicle at 45ms. At the same time, the occupant clearly started to move forward on the booster seat. At 80ms, the occupant rotated obviously toward to the door interior. The left foot of occupant contacted the frontal seat back and the occupant continued to rotate with the vehicle together at 102ms. At 112ms, the occupant's left lower leg and foot impacted the door interior. The right foot impacted the back of the frontal seat at 116ms. At 136ms, the contact between the left hand and the door interior could be found. After that time, the occupant began to rebound, at 186ms, the head impacted the foam of the headrest.

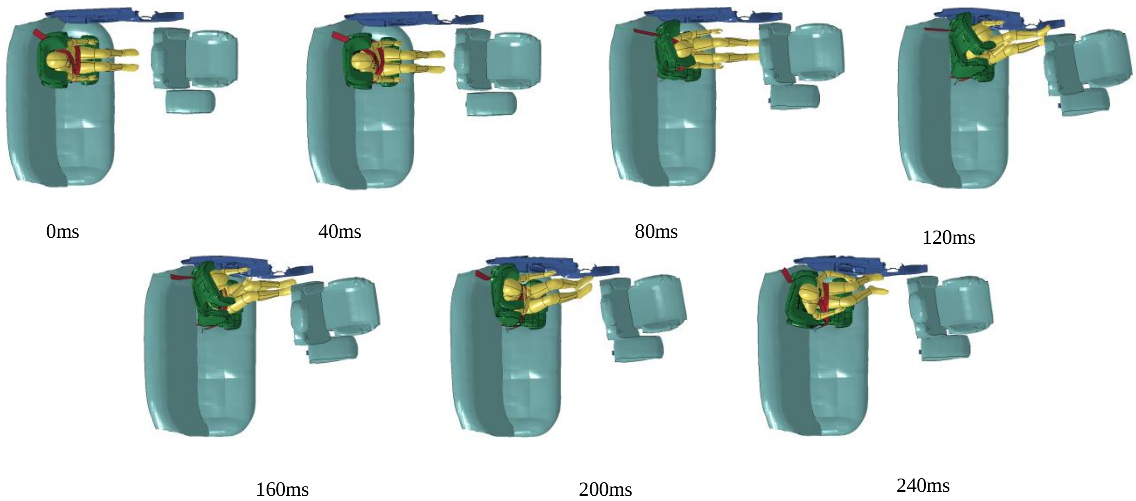

Figure 6 Occupant Kinematic Response (high-backed)

Figure 7 displays that the occupant different postures at the same time intervals in backless situation when the small overlap frontal impact was conducting. About at 32ms, the occupant started to move forward. At 88ms, the lap belt slid to the abdomen, the occupant showed the submarining, the shoulder belt left from the chest to the neck area. At 98ms, the left foot contacted the back of the frontal seat. The left forearm and hand impacted the door interior at 110ms. At 114ms, the right foot hit the frontal seat back. After that time, the occupant began to rebound, the head impacted the rear seat back at 178ms. At meantime, the shoulder belt left from the neck area, and arrived at face area at 194ms. In the rebound process, the left foot contacted the door interior at 204ms.

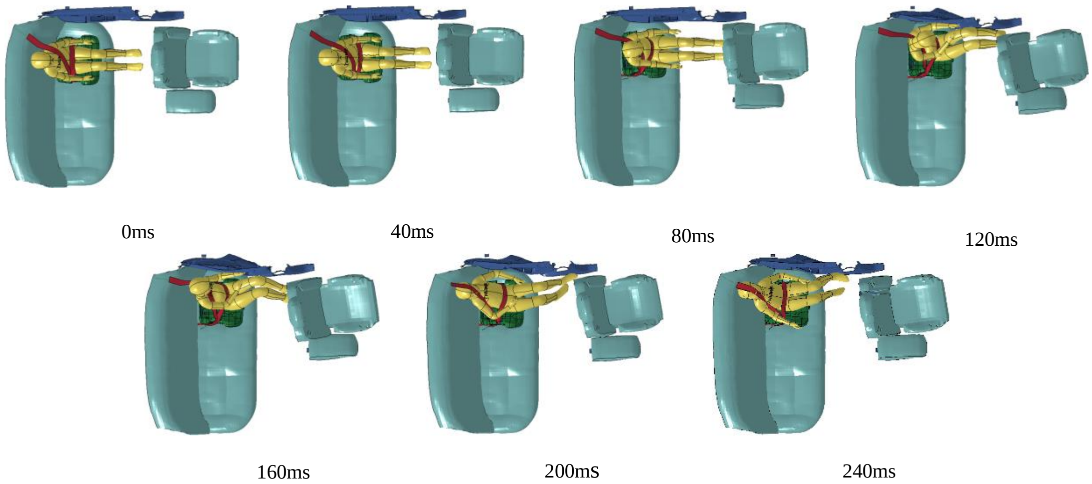

Figure7 Occupant Kinematic Response (backless)

The occupant kinematic response differences between the high-backed and backless situation are as following: First, submarining phenomenon appeared in backless situation. Second, the occupant head impacted heavily the rear seat back in backless situation during the second half of the crash. However, the head hit slightly the headrest foam in high-backed situation. Third, the shoulder belt left from the occupant chest area to the face area in backless situation. It was very dangerous for occupant who lost the restrained by the shoulder belt.

4.3 Injury Parameters

The time history curves of head resultant acceleration and chest resultant acceleration can be found in Figure 8 and Figure9. The head resultant acceleration in each situation was similar during the first half of the crash. But at about 180ms, the head resultant acceleration maximum value in backless situation was very higher than high-backed situation. According to the previous occupant kinematic response, the reason of this phenomenon is that the occupant head impacted heavily the rear seat back in the rebound process. Figure 9 shows that chest resultant acceleration was always higher in backless situation during the 100ms to 240ms. That the shoulder belt forces applied to the headrest and occupant chest in high-backed situation and only applied to the occupant chest in backless situation caused the phenomenon described before.

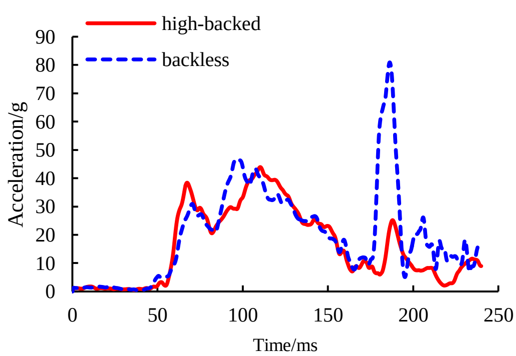

Figure8 Head Resultant Acceleration

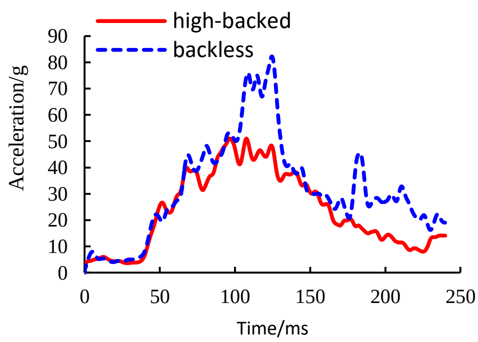

Figure9 Chest Resultant Acceleration

Table2 indicates the head resultant acceleration, HIC15, chest resultant acceleration, chest deflection and viscous criterion (VC). The corresponding IARVs (Injury Assessment Reference Values) were also displayed. The head acceleration, HIC15, chest acceleration and chest deflection were compared to IARVs reported by Mertz et al [5], the VC was compared to 1.0m/s published by Viano et al [6]. All injury parameters didn't exceed the IARVs except the chest deflection in both situations. Apart from VC value, other injury parameters were higher in backless situation than high-backed situation.

Table2

	Head Acc		Chest ACC	Chest Defl	VC
	Max/g	HIC15	Max/g	Max/mm	Max/m s^{-1}
IARV	189	723	93	31	1.0
High-backed	51.01	287.90	43.92	44.90	0.60
backless	80.91	471.80	82.22	46.60	0.52

4.4 Intracranial Pressure

Ward et al [7] found that severe brain injury occurs when the intracranial pressure exceeds 235KPa on the head impact side. The intracranial pressure clouds of the brain are showed in Figure 10. The maximum value of intracranial pressure in high-backed situation is 113.10KPa that head hitting the headrest foam caused. The main reason of the maximum intracranial pressure 162.60KPa occurring in backless situation is the head hitting the rear seat back. Because the intracranial pressure values are lower than 235KPa in both situations, severe brain injury don't emerge.

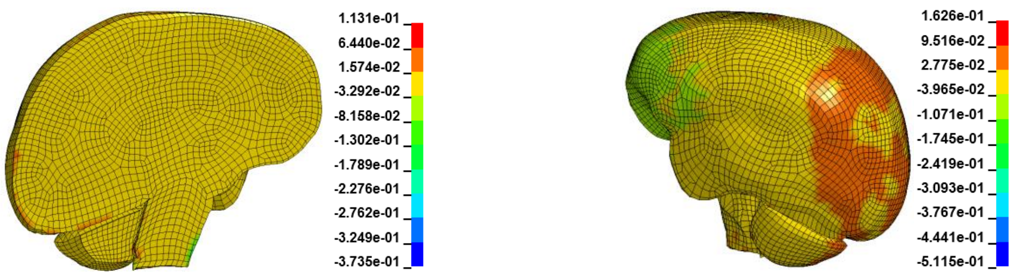

(a) high-backed **(b) backless**

Figure10 Intracranial Pressure Clouds

4.5 Brain Von Mises Stress

Baumgartner et al [8] corresponding research shows that it can cause brain concussion when brain tissue stress reaches 15-20KPa. The maximum value of Von Mises stress of brain is 8.73KPa and 11.94KPa respectively in high-backed and backless situations. So the brain concussion will not appear.

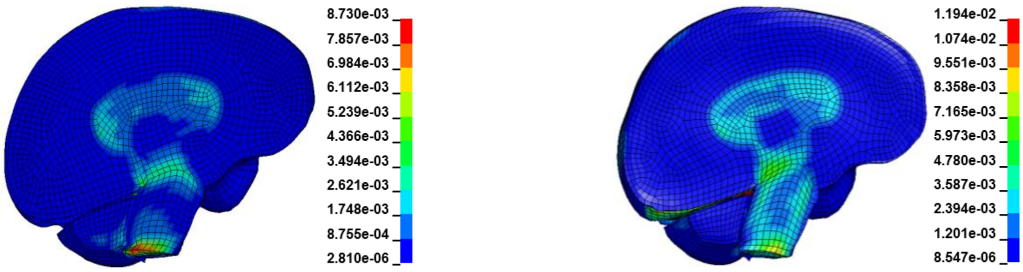

(a) high-backed **(b) backless**

Figure11 Brain Von Mises Clouds

4.6 Brain Shear Stress

Liying Zhang et al [9] found that brain shear stress level were 6.0, 7.8, and 10.0KPa for 25%, 50% and 80% probability of mild traumatic brain injury(MTBI). The maximum value of shear stress 4.91KPa and 6.82KPa be found in their respective own situation. It can be concluded that MTBI may happen to the occupant in backless situation.

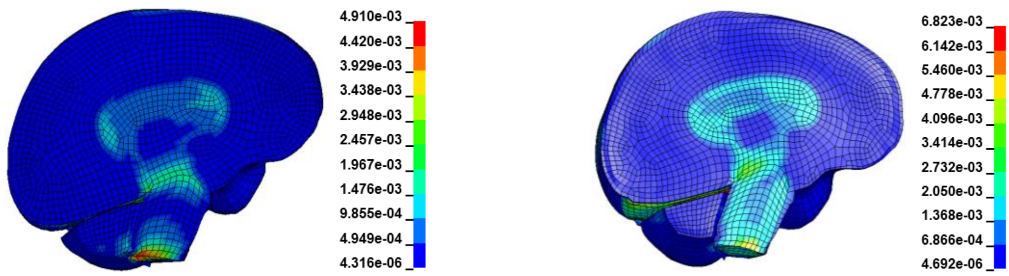

(a) high-backed **(b) backless**

Figure12 Brain Shear Stress Clouds

4.7 Ribs

LV Wenle et al [10] scaled the ultimate strain of adult rib cortical bone and found that the ultimate strain of children rib cortical bone ranged from 3.6% to 4.5%. Figure 13 displays the first principle strain of ribs. The maximum value of the first principle strain is 42.91% in high-backed situation. The reason why third rib experienced high risk of fracture was constriction from shoulder belt. The maximum value of the first principle strain 58.17% appears in backless situation because the shoulder belt slid to neck area and pressed the ribs here. So the fracture risk of the first, second and third ribs was high.

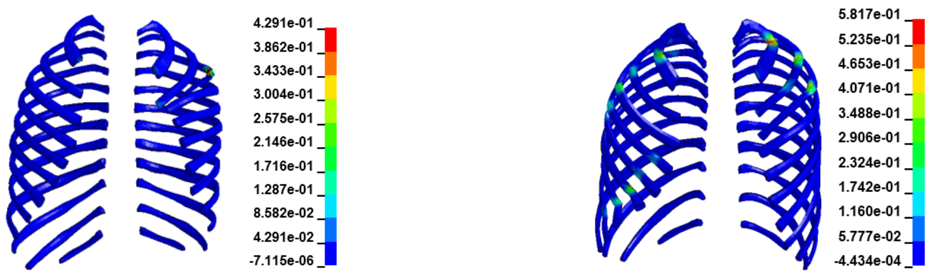

(a) high-backed **(b) backless**

Figure13 Rib the First Principle Strain Clouds

4.8 Heart

YAMADA et al [11] researched that the ultimate tensile strain of myocardial tissue of 0 to 9-year-old child is 62.9 ± 6.9%, and the first principal strain tolerance limit of the heart contusion is 30%. Figure 14 indicates the first principal strain cloud of the occupant heart in both situations. It can be seen from the strain clouds that the maximum first principal strain of high-back and no back is 54.21% and 51.62% respectively. The results show that the occupant heart in both situations may be at risk of contusion.

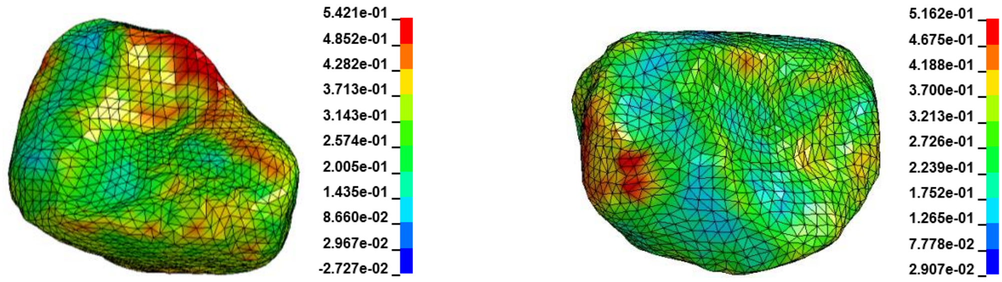

(a) high-backed **(b) backless**

Figure14 Heart the First Principle Strain Clouds

4.9 Lung

GAYZIK et al [12] used the animal (mouse) test CT scan and simulation to point out that the first principal strain can be used to predict lung injury better and the threshold of the first principal strain injury is about 35% in lung tissue injury in the finite element model. The maximum value of lung the first principle strain is 143.90% and 154.30% from Figure 15 in their own situation respectively. Therefore lung contusion may occur.

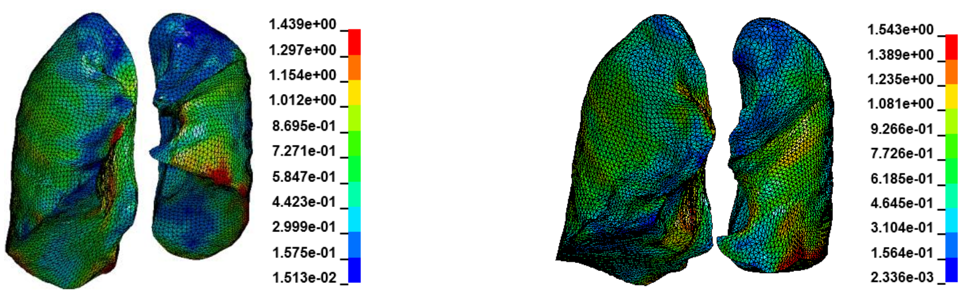

(a) high-backed **(b) backless**

Figure15 Lung the First Principle Strain Clouds

5 Conclusions

In this paper, the injury risk of 6YO child occupant in small overlap frontal impact was investigated by using finite element simulation. The submarining phenomenon appeared and shoulder belt slipped off in backless situation. The 6YO occupant experienced low injury risk of head and high risk of rib fracture, heart contusion and lung contusion in both situations. Moreover, the injury risk of 6YO occupant is higher in backless situation than high-backed situation.

6 Acknowledgements

The authors would like to acknowledge support of the National Natural Science Foundation of China (Project No: 51675454), the Natural Science Foundation of Fujian Province, China (Project No: 2016J01748).

References

[1] M Lindquist, A Hall, et al. Car structural characteristics of fatal frontal crashes in Sweden[J]. International Journal of Crashworthiness, 2004, 9 (6):587-597.

[2] Jason J, Hallman et al. Injury Differences Between Small and Large Overlap Frontal Crashes [C] //55th Annals of Advances in Automotive Medicine Conference, 2011.

[3] L Cao, P Zhang, L Yan, et al. A Study on Driver Injury in Oblique and Small Overlap Crashes Under Car to Car Collision [J]. Automotive Engineering, 2016, 38(2):174-180.

[4] Cao Libo, Zhang Ruifeng, et al. Study on the Child Passenge Injury Mechanism and Protection [J]. Chinese Journal of Automotive Engineering, 2012, 2 (1): 16-23.

[5] Harold J, Annetle L.Irwin. Biomechanical and Scaling Bases for Frontal and Side Impact Injury Assessment Reference Values [J]. Stapp Car Crash Journal, 2003, 47:155-188

[6] Viano DC, Lau IV.Thoracic Impact: A Viscous Tolerance Criterion [C]// SAE Technical Paper 856025, England: 1985, 104-114.

[7] Ward C, Chan M, et al. Intracranial pressure-a brain injury criterion [C]//Proceedings of Twenty-fourth Stapp Car Crash Conference, 1980:161-185.

[8] Baumgartner D, Willinger R et al. Tolerance limits for mild traumatic brain injury derived from numerical head impact replication[C]//Proceedings of the 2001 International IRCOBI Conference on the Biomechanics of Impacts, 2001:353-355.

[9] Liying Zhang, King H. Yang et al. A Proposed Injury Threshold for Mild Traumatic Brain Injury [J]. Journal of Biomechanical Engineering, 2004, 126(2):226-236.

[10] LV Wenle, RUAN Shijie, LI Haiyan, et al. Development and Validation of a 6-year-old Pedestrian Thorax and Abdomen Finite Element Model and Impact Injury Analysis[J]. International Journal of Vehicle Safety. 2015, 8(4): 339-356.

[11] Yamada H. Strength of biological materials [M]. Williams & Wilkins, 1970.

[12] GAYZIK F S. Development of a Finite Element Based Injury Metric for Pulmonary Contusion [D].Winston-Salem, North Carolina: Wake Forest University, 2008.